



Heat transfer and friction factor characteristics using continuous M shape ribs turbulators at different orientation on absorber plate solar air heater

Sachin Chaudhary¹, Varun¹, Manish Kumar Chauhan²

¹ Department of Mechanical Engineering, NIT Hamirpur-177005, India.

² Department of Mechanical Engineering, College of Engineering Roorkee, Roorkee-247667, India.

Abstract

This paper having more concern with enhancement of heat transfer coefficient using artificial roughened absorber plate on solar air heater. The increment in heat transfer also leads to increase in friction factor which leads to increase in pumping power. In this study M shape geometry has been studied which is having different orientation. The effect of roughness parameters relative roughness height (e/D), relative roughness (P/e) and angle of attack (α) on Nusselt number and friction factor have been seen. The range of Reynolds number 3000-22000, e/D , P/e and α are 0.037-0.0776, 12.5-75 and 30-60° respectively. It has been found out that providing the artificial roughness of M shape increases heat transfer upto 1.7-1.8 times over the smooth duct.

Copyright © 2012 International Energy and Environment Foundation - All rights reserved.

Keywords: Friction factor; Nusselt number; Roughness geometry parameters; Solar air heater.

1. Introduction

It is well known that population of the world is increasing exponentially. For performing any task energy is required. There are limiting conventional source of energy (coal, oil and gases) available in world and all these sources are depleting day by day. Because of huge demand of energy, it would not be possible to meet the energy requirement up to next few years by conventional sources. So, it is necessary to find the other alternative source of energy. Out of all sources of renewable energy, solar energy has many advantages over others. It is the cheapest and easily available source having in abundant.

Solar energy has many applications such as cooking, fruits and vegetables drying, water and air heating industries, power generation etc. The best possible way to harness solar energy is to convert it into thermal energy and utilized for desired purposes. Conventional solar air heater is one of the basic equipment through which solar energy is converted into thermal energy. It has been observed that the thermal performance of the conventional solar air heater is poor because of the following reasons:

- Low convective heat transfer between the absorber plate and air.
- Low heating capacity of air.
- Formation of the sub-viscous layer near the absorber plate.

The basic schematic diagram of single pass conventional solar air heater is given in Figure 1 [1].

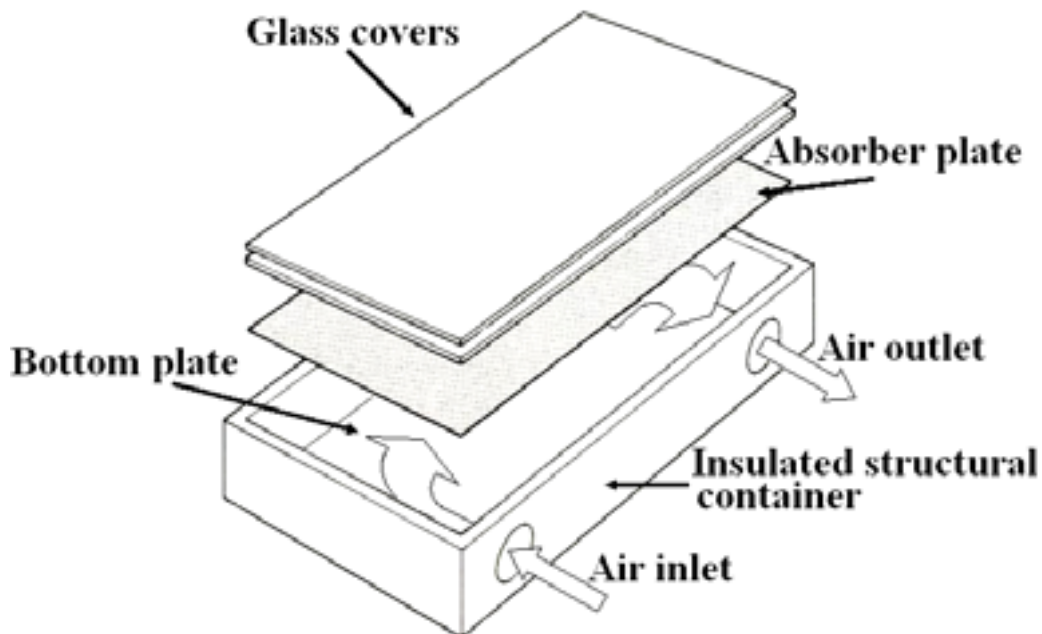


Figure 1. Schematic view of solar air heater [1]

As we know that when a fluid comes in contact with the stationary absorber plate, a thin viscous sub-layer develops adjacent to its wall in turbulent boundary layer. So, the heat transfer between air and absorber plate get reduced. The heat transfer between absorber plate and air can be enhanced either by increasing the heat transfer surface area using extended and corrugated surface or by increasing the convective heat transfer coefficient. The easiest and simplest way to do is that artificial turbulators are to be created on the underside of the absorber plate. The artificial roughness may be created either by sand blasting, sand graining or by use of regular fixed wire geometric roughness. The artificial roughness breaks up the laminar boundary layer of flow and transform in to turbulent flow. It is ,therefore desirable that the turbulence must be created near the heat transferring surface and break the viscous sublayer for augmenting the heat transfer However, it also increase the pressure drop due to increase in friction.

It is most commonly used device in solar energy. Applications include, drying of agriculture products, space heating, seasoning of wood, curing of industrials products.

Several investigators have been proposed that the provision of artificial roughness on underside of absorber plate could substantially enhance the heat transfer rate of solar air heater. Prasad and Saini [2, 3] has been developed Nusselt number and friction factor correlation for protruded wire which is fixed to the underside of absorber plate. Han et al [4-7] performed experimentation study to see the effect of rib shape, pitch height ratio, spacing in square rib shape and angle of attack on heat transfer and friction factor. Vaun et al. [8] investigated heat transfer and friction factor characteristics of combined transverse as well inclined ribs as roughness element on absorber plate. Momin et al. [9] carried out the experimentation study to see the effect of V-shaped ribs as roughness element of absorber plate. Muluwork et al. [10, 11] reported the comparison of thermal performance for roughened absorber plate which is having staggered discrete V-apex (up and down). Saini and Saini [12] reported the effect of arc shaped ribs on heat transfer and fluid flow characteristics of rectangular duct of solar air heater. Aharwal et al. [13] has been investigated the effect of artificial roughened absorber plate, having integral non-continuous ribs arrangement. Karwa et al. [14, 15] studied the effect of integral chamfered ribs as roughness element on absorber plate of solar air heater. Karmare and Tikekar [16] reported an experimental investigation and developed correlation for heat transfer coefficient and friction factor for metal grit ribs as roughness element on absorber plate.

Jaurker et al. [17] and Layek et al. [18] carried out an experiments and investigated heat transfer and friction characteristics for repeated integral transverse ribs-grooved and transverse chamfered rib- groove roughness on absorber plate respectively. Verma and Prasad [19] investigated the effect of transverse wire roughness on heat and flow characteristics of two roughened collectors and one plane surface collector. Saini and Verma [20] reported heat transfer characteristics for dimpled shape as roughness geometry on absorber plate. Karmare and Tikekar [21] reported CFD analysis of fluid flow and heat

transfer in metal grit ribs as roughness element on absorber plate. Bopche and Tandale [22] performed experimental investigation on heat transfer and friction characteristics of a turbulator roughened solar air heater duct and also, developed correlations for the same. Bhushan and Singh [23] have given the correlation for Nusselt number and friction factor for solar air heater duct having artificially roughened absorber plate. Promvonge and Thianpong [24] studied the thermal performance of turbulent channel flows over different shape ribs. Moreover, Kumar and Saini [25] also analyzed performance of solar air heat duct provided artificial roughness through CFD tool. Lee et al. [26] performed detailed measurement of heat / mass transfer with continuous and multiple V-shaped ribs in rectangular channel. Eiamsa-ard et al. [27] have seen the effect of peripherally-cut twisted tape insert on heat transfer and thermal performance characteristics in laminar and turbulent flows. Promvonge et al. [28] investigated the enhancement of heat transfer in triangular ribbed channel with longitudinal vortex generators. Aharwal et al. [29] reported heat transfer and fluid flow in rectangular duct with inclined discrete ribs. Hans et al. [30] investigated heat transfer and friction factor correlations for solar air heater duct roughened artificially with multiple V- ribs. Mittal et al. [31] studied the effective efficiency of solar air heaters having different types of roughness elements on absorber plate.

2. Experimental setup

An experimental set-up has been designed and fabricated as per the ASHRAE standard [32]. A schematic layout experimental setup is shown in Figures 2 and 3. The schematic diagram of experimental setup consists of three sections, an entry section, test section and outlet section respectively. The rectangular duct is 1375 mm × 287 mm × 197 mm and fabricated with the red marandi wood and 19 mm thick plywood panel. The test section is of 1000 mm long and 14 mm in height. The entry and exit section length were 250 mm and 125 mm respectively. ASHRAE standard 97-77 [32] recommends the minimum entry and exit length of $5\sqrt{(WH)}$ and $2.5\sqrt{(WH)}$, i.e 236.6 mm and 118.3 mm. After outlet section, a plenum was also provided for the proper mixing of air. The entrance and exit section length is covered with 19 mm thick plywood panel glued with sunmica. The three walls (two sides and a bottom) of test section is finished with white sun mica and a 8 mm thick artificial roughened aluminium absorber plate acts top wall of test section. The upper side of the absorber plate painted black to absorb more heat radiation. The artificial roughness has been provided by gluing desired aluminium wire on the underside of the absorber plate.

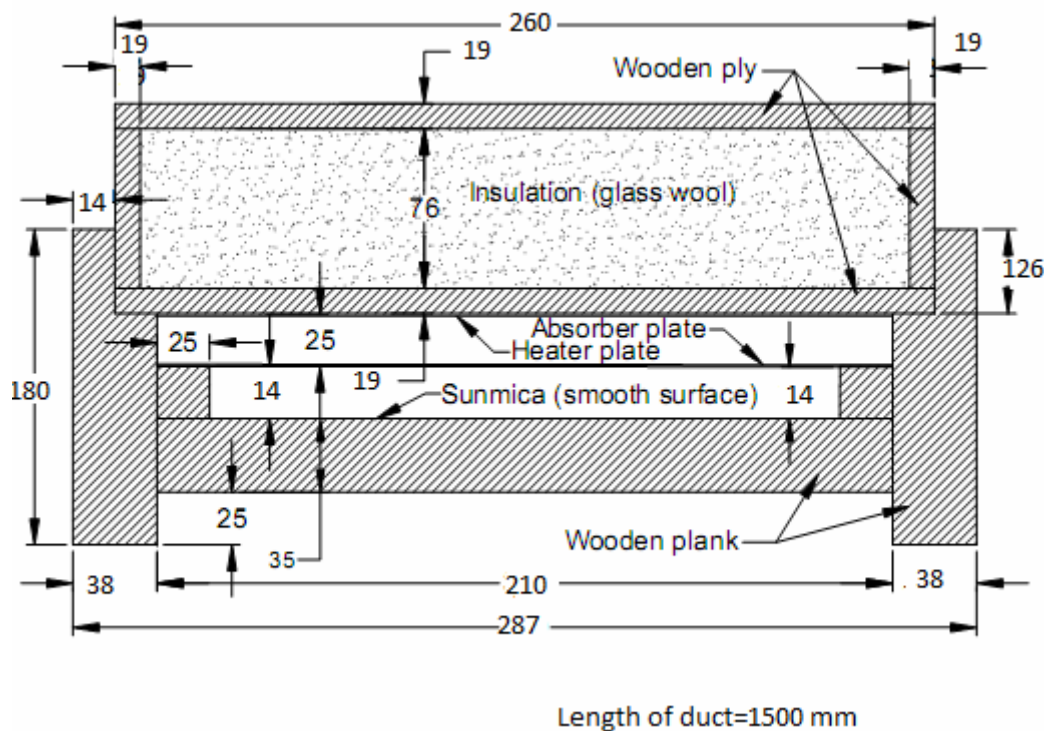
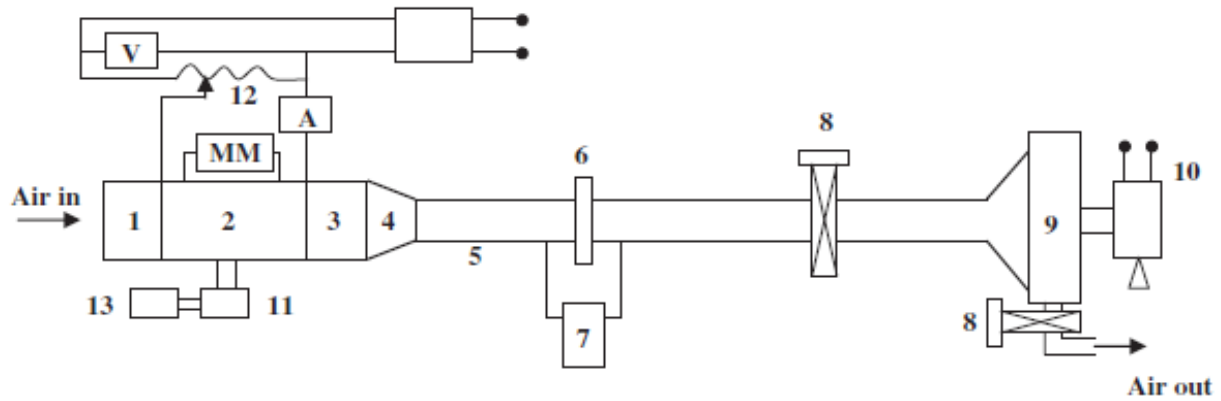
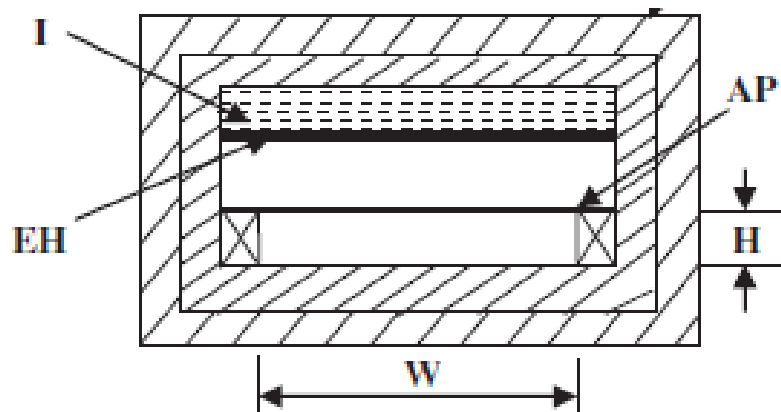


Figure 2. Sectional view of solar air rectangular duct



(a)



(b)

- | | |
|---------------------------|---------------------|
| 1. Entry Section | I –Insulation |
| 2. Test Section | AP- Absorber Plate |
| 3. Exit Section | H- Duct Height |
| 4. Mixing Plenum | W-Duct Width |
| 5. G.I Pipe | E-Electric Heater |
| 6. Orifice Plate | A-Ammeter |
| 7. U-tube Manometer | V-Voltmeter |
| 8. Control Valves | MM- Micro Manometer |
| 9. Centrifugal Blower | |
| 10. Electric Motor | |
| 11. Selector Switch | |
| 12. Voltage Variac | |
| 13. Temperature Indicator | |

Figure 3. (a) Schematic view of experimental apparatus of solar air heater (b) Sectional view of duct

An electric heater 1000 mm × 160 mm is made of nichrome wire which is having parallel and series loops. The electric heater was mounted on 4 mm thick asbestos sheet at the backside of duct cover which was made of 19 mm thick plywood panel. A mica sheet is placed between asbestos sheet and electric heater. The glass wool insulation density 50 kg/m³ was filled in the cover to minimize the heat losses. The heater is placed 25mm above the roughened absorber plate. The range of roughness and flow parameters is listed in Table 1.

Table 1: Range of roughness and flow parameters

Parameters	Range
Roughness height, e	1mm, 1.5mm, 2 mm (3values)
Rib pitch, P	25mm, 50 mm, 75 mm (3 values)
Rib Width ,w	100 mm
Relative Roughness height (e/D _h)	0.03884-0.07768 (3values)
Duct Aspect ratio (W/H)	11.43
Angle between geometry 'α'	30-60° (3 values)
Reynolds Number (Re)	3000-22000
Solar Insolation (I)	1000 W/m ²

2.1 Instrumentations

2.1.1 Temperature measurement

Calibrated 28 SWG copper-constantan thermocouples were used to measure the air temperature and absorber plate temperature. Four thermocouples were inserted from the bottom in the test section of duct to measure the average temperature of air flowing through it. Twelve more thermocouples are mounted on the upper side of the absorber plate to measure average temperature of the absorber plate.

2.1.2 Air flow measurement

To measure the mass flow rate through the rectangular duct orifice meter has been used. The orifice meter is calibrated by using the Pitot tube and the value of co-efficient of discharge (C_d) was obtained as 0.62. Pressure drop across the orifice meter was measured by means of a U-tube manometer.

2.2 Parameter measurement

The following parameters are to be measured for performance analysis of roughened solar air heater.

- Temperature of heated absorber plate and temperature of air at inlet and outlet.
- Pressure drop across the test section.
- Pressure drop across the orifice meter.

3. Data reduction

The various steps in the computation of Nusselt number and Friction factor have been explained below:

Step I: Calculation of mass flow rate, using the following equation:

$$m = C_d A_o \left[\frac{2\rho\Delta P_o}{1 - \beta^4} \right]^{0.5} \quad (1)$$

where m is mass flow rate (kg/s), C_d is coefficient of discharge, A_o is cross-section area of orifice (m²), β is ratio of orifice diameter to pipe diameter (D/d).

$$\Delta P_o = 9.81\rho_m\Delta h_o \sin \theta \quad (2)$$

where Δh_o is the difference of manometric fluid levels in U-tube manometer (m).

For a particular mass flow rate, the velocity of flow (V) is calculated by;

$$V = \frac{m}{\rho WH} \quad (3)$$

where V is velocity of air (m/s), W is width of duct (m), H is height of duct (m).

For the calculated value of velocity (V), Reynolds number is given as;

$$Re = \frac{\rho VD}{\mu} \quad (4)$$

where Re is Reynolds number, ρ is density of air (kg/m^3), D is hydraulic diameter of duct (m), μ is dynamic viscosity.

Step II: The useful heat gained by air is calculated through

$$Q_u = mC_p(T_o - T_i) \quad (5)$$

where Q_u is useful heat gain rate (W), C_p is specific heat of air at constant pressure (J/kgK), T_i is inlet temperature of air (K), T_o is outlet temperature of air (K).

Step III: The heat transfer coefficient is to be calculated by

$$h = \frac{Q_u}{A_p(T_p - T_f)} \quad (6)$$

where h is convective heat-transfer coefficient ($\text{W/m}^2\text{K}$), T_p is average plate temperature (K), T_f is mean temperature of air (K), A_p is area of absorber plate (m^2).

Step IV: The Nusselt number is calculated by using the following equation;

$$Nu = \frac{hD}{k} \quad (7)$$

where Nu is Nusselt number of roughened duct, k is thermal conductivity of air (W/mK).

Step V: The friction factor is calculated by using the following equation;

$$f = \frac{2\Delta P_d D}{4\rho L V^2} \quad (8)$$

where ΔP_d is Pressure difference of water column levels in micromanometer (m), L is test section length for pressure drop measurement (m).

Based on error analysis for different instruments used in data collection [33], the uncertainties has been calculated for Reynolds number, Nusselt number and Friction factor is ± 1.01 , 3.32 and 1.04% respectively.

4. Validity test

Both Nusselt number and friction factor calculated from the experimental data for smooth duct and also compared their values with the values obtained from Dittus –Boelter equation (9) and Modified Blasius equation (10) for Nusselt number and friction factor, respectively. The friction factor values are also compared with Karman- Nikuradse equation (11).

- Dittus -Boelter Equation:

$$Nu_s = 0.023 Re^{0.8} Pr^{0.4} \quad (10^4 \leq Re \leq 1.24 \times 10^5) \quad (9)$$

- Modified Blasius Equation:

$$f_s = 0.085 Re^{-0.25} \quad (4 \times 10^3 \leq Re \leq 10^5) \quad (10)$$

- Karman- Nikuradse Equation:

$$f_s = 0.046 Re^{-0.2} \quad (3 \times 10^4 \leq Re \leq 10^6) \quad (11)$$

The comparison in predicated and experimental values of Nusselt number and friction factor has been shown in Figures 4 and 5 respectively.

It has been found out that deviation occurred in predicated and experimental values is of the order of $\pm 6.7\%$ and $\pm 3.3\%$ for Nusselt number and friction factor respectively.

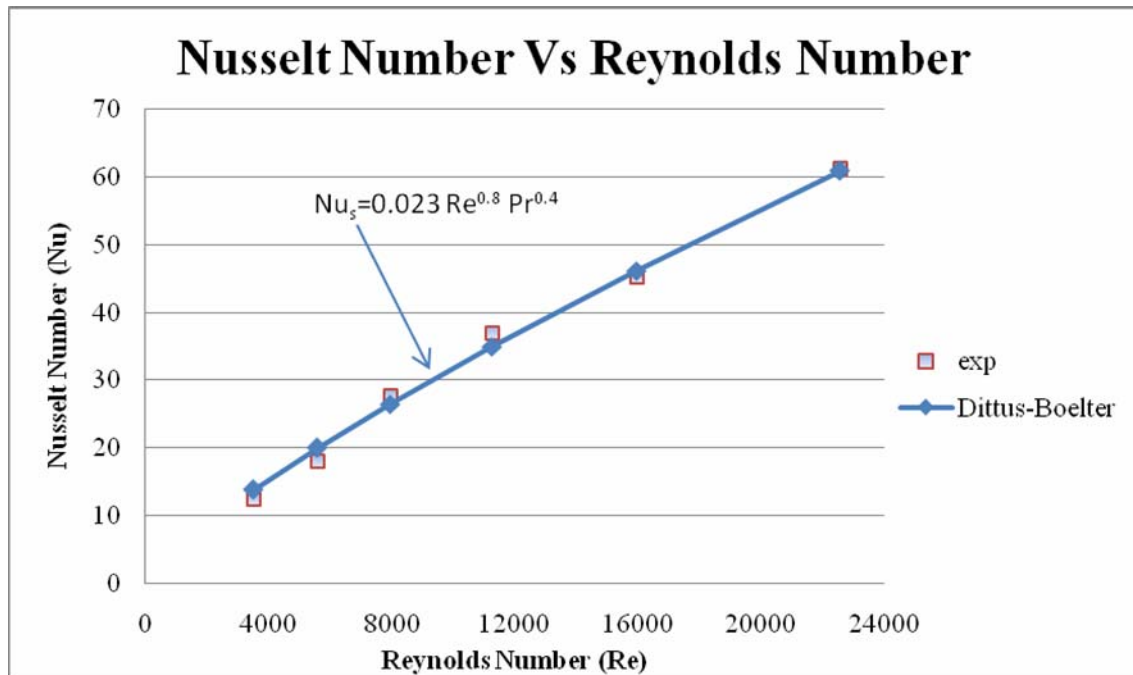


Figure 4. Comparison of experimental and predicted values of Nusselt number for smooth duct

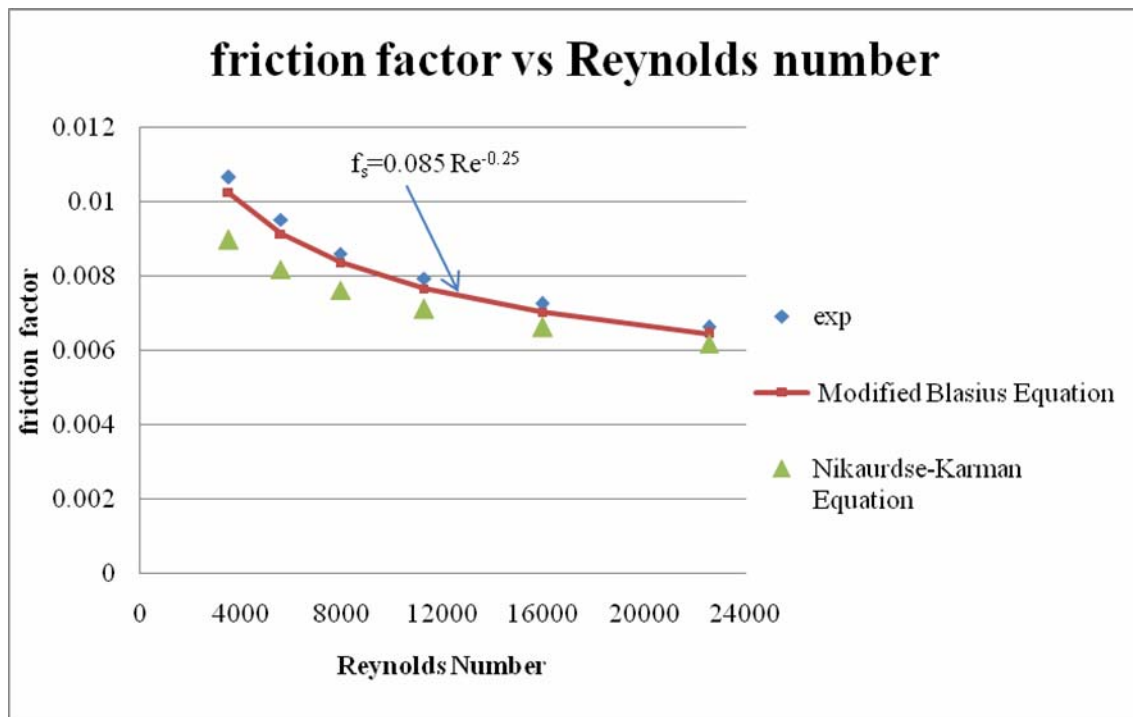


Figure 5. Comparison of experimental and predicted values of friction factor for smooth duct

5. Result and discussion

5.1 Nusselt number (Nu)

The Nusselt number (Nu) is plotted as function of Reynolds number (Re) for all absorber plates having different orientation of roughness geometry. The Nusselt number increases with increase in Reynolds number which is shown in Figures 6-8. The maximum value of Nusselt number attains corresponding to e/D , P/e and α are 0.0777, 25 and 60 respectively. As we know that higher the Nusselt number higher would be the heat transfer coefficient (h).

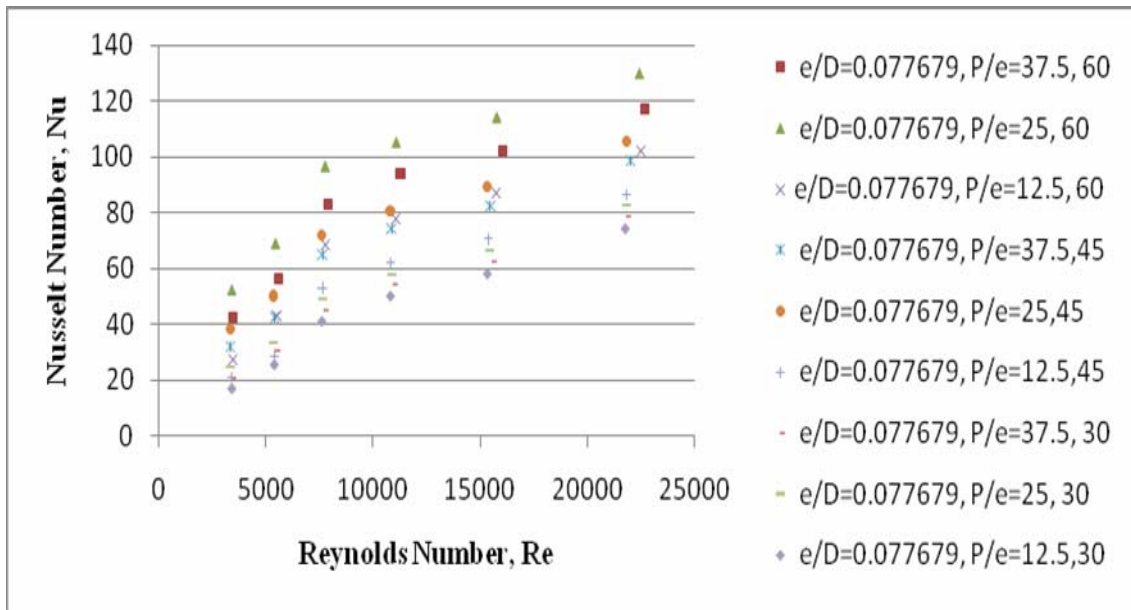


Figure 6. Variation of relative roughness height ($e/D=0.077679$) on Nusselt number

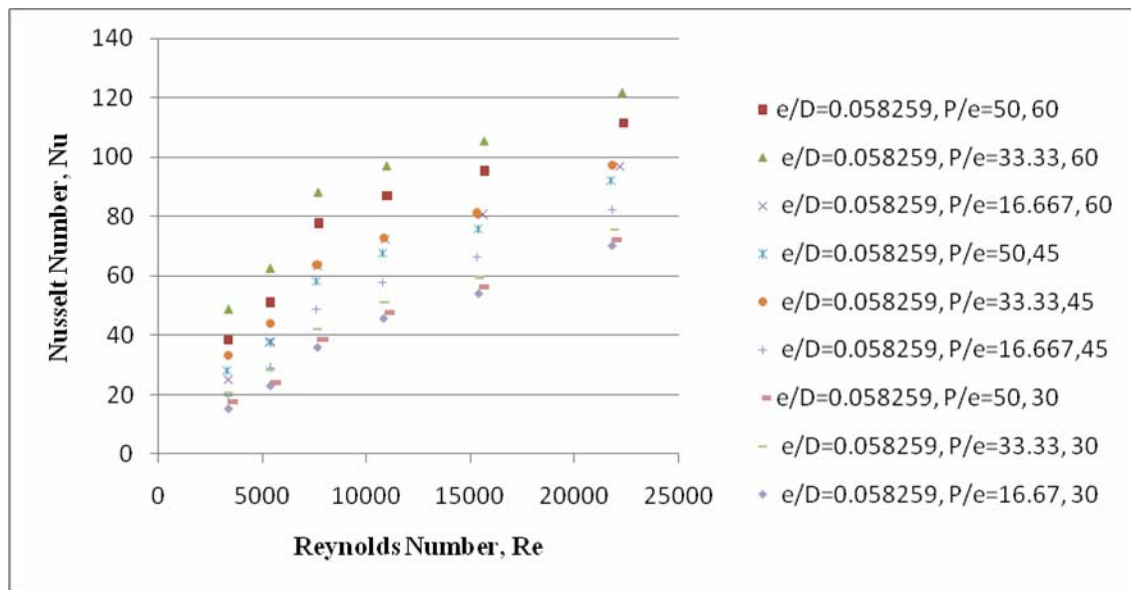


Figure 7. Variation of relative roughness height ($e/D=0.058259$) on Nusselt number

5.1.1 Effect of relative roughness height (e/D)

It is observed from figures that the Nusselt number increases with the increase in rib height. This effect can be attributed to the fact that as e/d increases, Nusselt number also increases. Further, if the roughness height is less than the thickness of laminar sub-layer then there will not be any enhancement in heat transfer. Thus, maximum rib height should be such that the fin and flow passage blockage effects are negligible. Figure 9 shows the behavior of three different relative roughness heights (e/D) for same value relative roughness pitch (P/e) 50 and angle of attack (α) 60° . Moreover, it is concluded that as the relative roughness height increases, Nusselt number also increases. But if it exceed beyond the height of boundary layer then it will not helpful in making the reattachment point. So, after this height Nusselt number start decreasing and ribs will act as fins. In Figure 9 the maximum Nusselt number would be at $0.0777(e/D)$ for different Reynolds number.

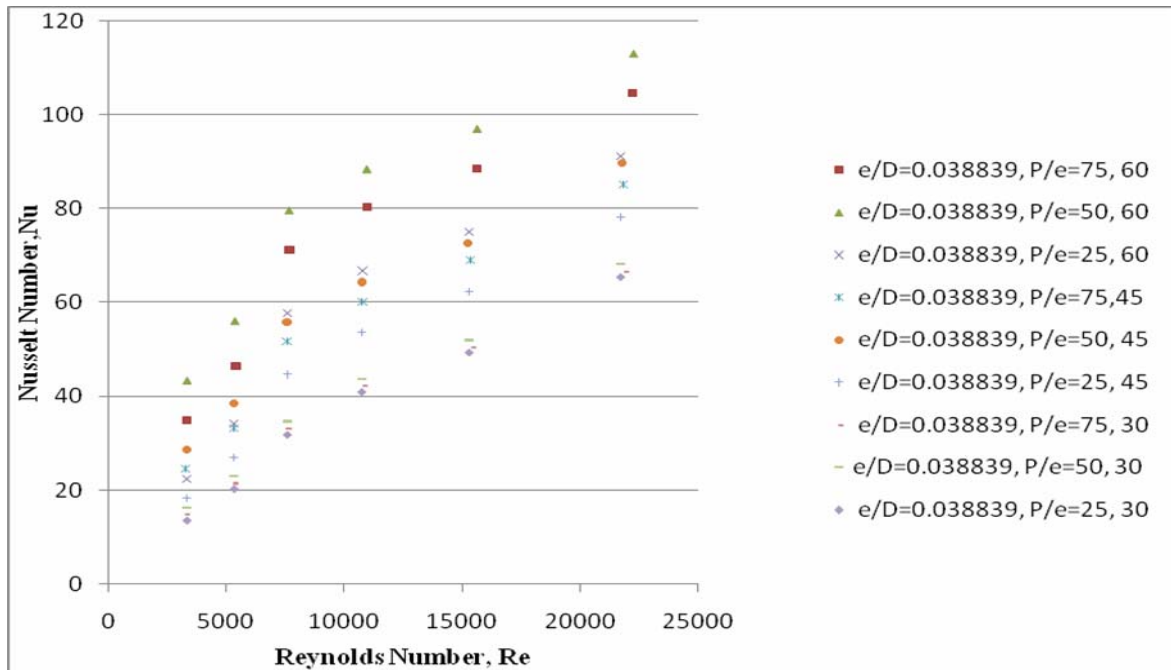


Figure 8. Variation of relative roughness height ($e/D=0.038839$) on Nusselt number

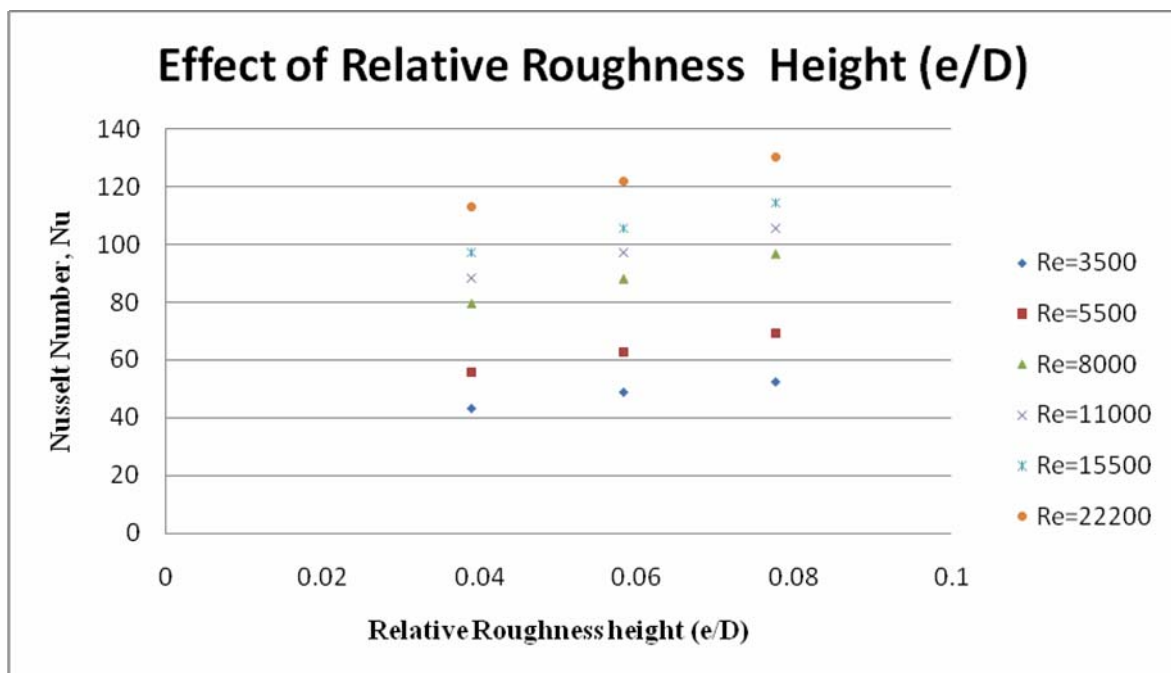


Figure 9. Effect of relative roughness height (e/D) on Nusselt number

5.1.2 Effect of relative roughness pitch (p/e)

Figure 10 shows the variation of Nusselt number with relative roughness pitch (P/e) parameters for the considered geometry. It has been observed that with the increase in the value of P/e , Nusselt number of considered geometries decreases. This is explained on the basis of flow separation. For higher P/e the flow which separates after each rib does not reattach before it reaches the succeeding rib. Also, maximum heat transfer has been found to occur in the vicinity of a reattachment point. The maximum heat transfer occurred at (P/e) 25 because of higher Nusselt number at higher Reynolds number. Hence, heat-transfer coefficient will maximum at the same value.

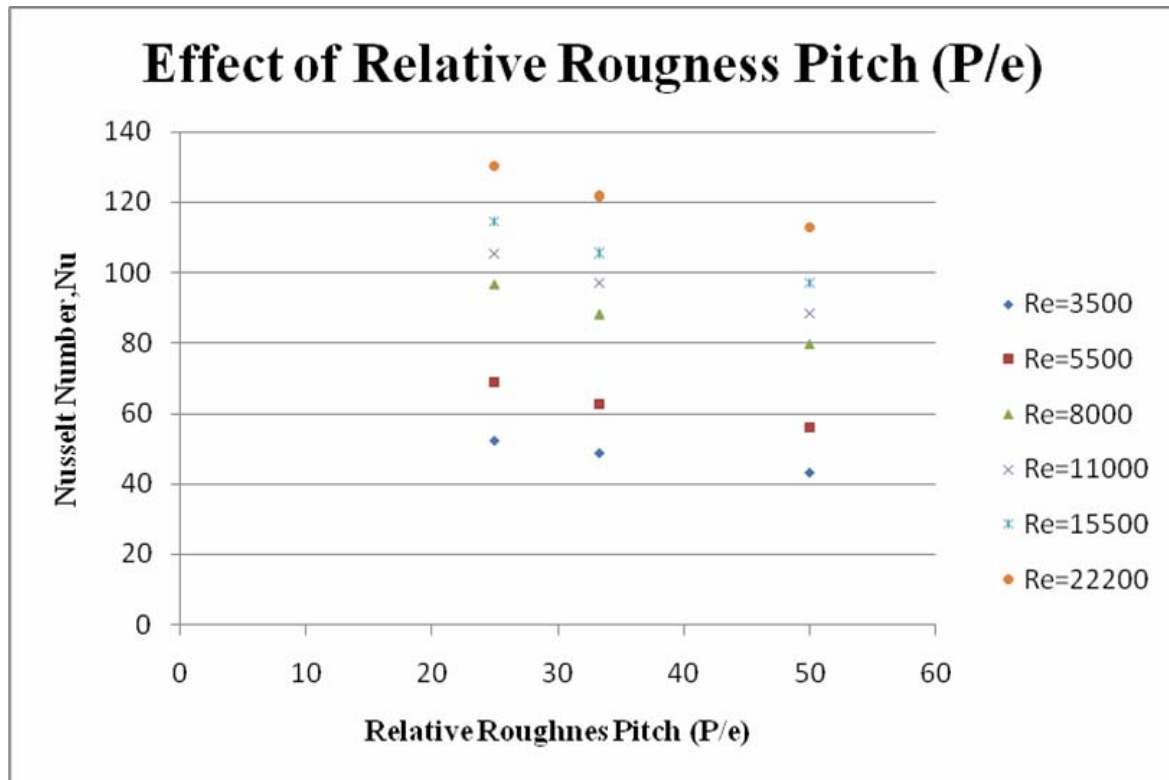


Figure 10. Effect of relative roughness pitch (P/e) on Nusselt number

5.1.3 Effect of angle of attack (α)

The variation of Nusselt number with the angle of attack for different Reynolds number is shown in Figure 11. It has been observed that the Nusselt number increase with the angle of attack and maximum value of it lies at 60° . The reason for this phenomenon may be separation of flow resulting from the presence of M shape continuous ribs.

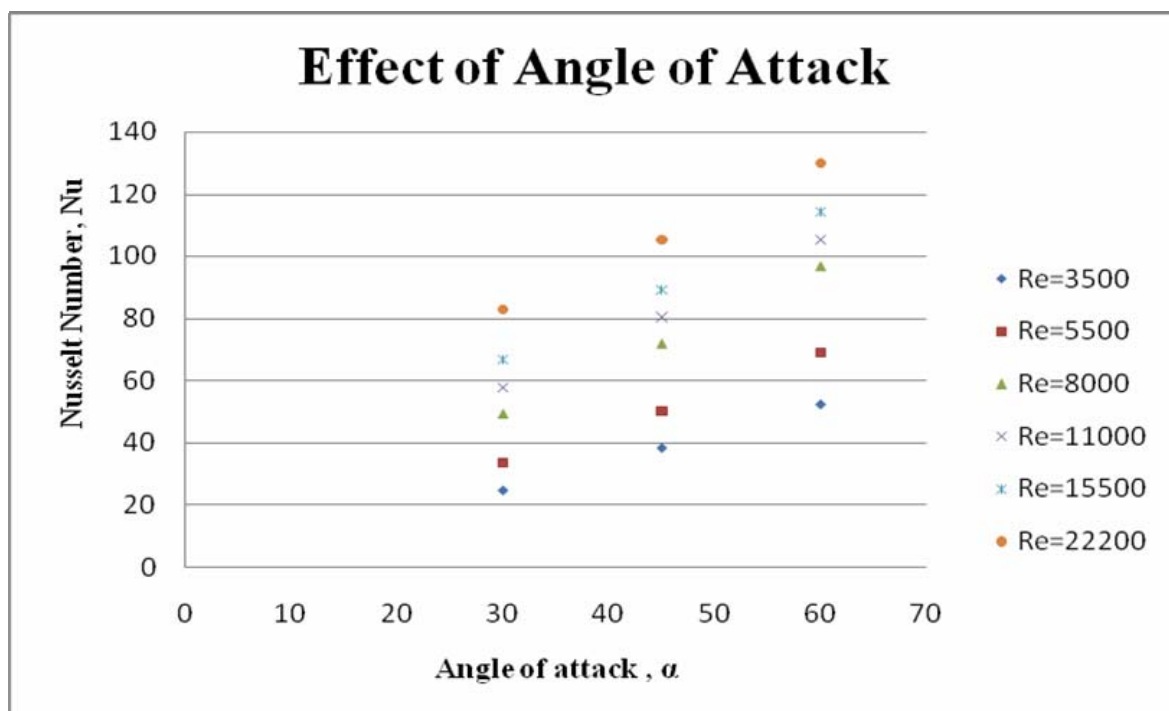


Figure 11. Effect of angle of attack (α) on Nusselt number

5.2 Friction factor (f)

The friction factor (f) is plotted as function of Reynolds number (Re) for all absorber plates having different orientation of roughness geometry. Figures show the general trend of the Nusselt number for all roughened absorber plate. The friction factor decreases with increase of Reynolds number. But, maximum value of Nusselt number attains corresponding to e/D , P/e and α is 0.077, 12.5 and 45° respectively. As we know that lower the Reynold number higher would be the friction factor (f).

5.2.1 Effect of relative roughness height (e/D)

Figures 12-14 show the variation of friction factor with relative roughness height (e/D) parameter for constant value of relative roughness height (e/D). It has been observed from these figures that the friction factor increases with the increase in rib height. This effect can be attributed to the fact that as e/D increases, friction factor also increases. Further, if the roughness height is less than the thickness of laminar sub-layer then there will not be any enhancement in heat transfer. Thus, maximum rib height should be such that the fin and flow passage blockage effects are negligible.

Figure 15 shows the behavior of three different relative roughness heights (e/D) for the same value of relative roughness pitch (P/e) 50 and angle of attack (α) 60° . Moreover, it has been concluded that as the relative roughness height increases, friction factor increases. But if it exceed beyond the height of boundary layer then it will not helpful in making the reattachment point. So, after this height friction factor further start increasing and ribs will act as fins. In Figure 12 friction factor would be maximum for 0.077 (e/D) for different Reynolds number.

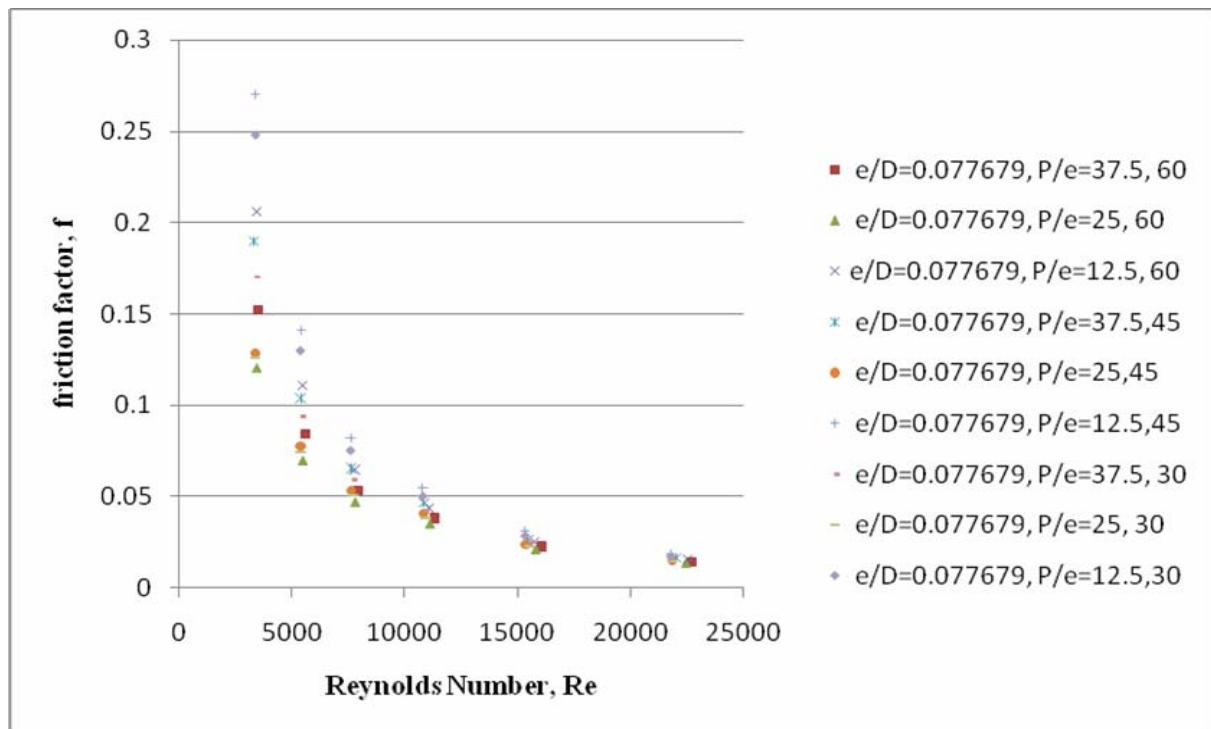


Figure 12. Variation of relative roughness height ($e/D=0.077679$) on friction factor

5.2.2 Effect of relative roughness pitch (P/e)

Figure 16 shows the variation of friction factor with relative roughness pitch (P/e) parameters for considered geometry. It has been observed that with increase in the value of P/e , friction factor of considered geometries decreases. This is explained on the basis of flow separation. For higher P/e the flow which separates after each rib does not reattach before it reaches the succeeding rib. Also, pressure drop has been found to occur in the vicinity of a reattachment point. The maximum pressure drop occurred at (P/e) 25 because of higher friction factor at lower Reynolds number. Hence, friction factor will maximum at the same value.

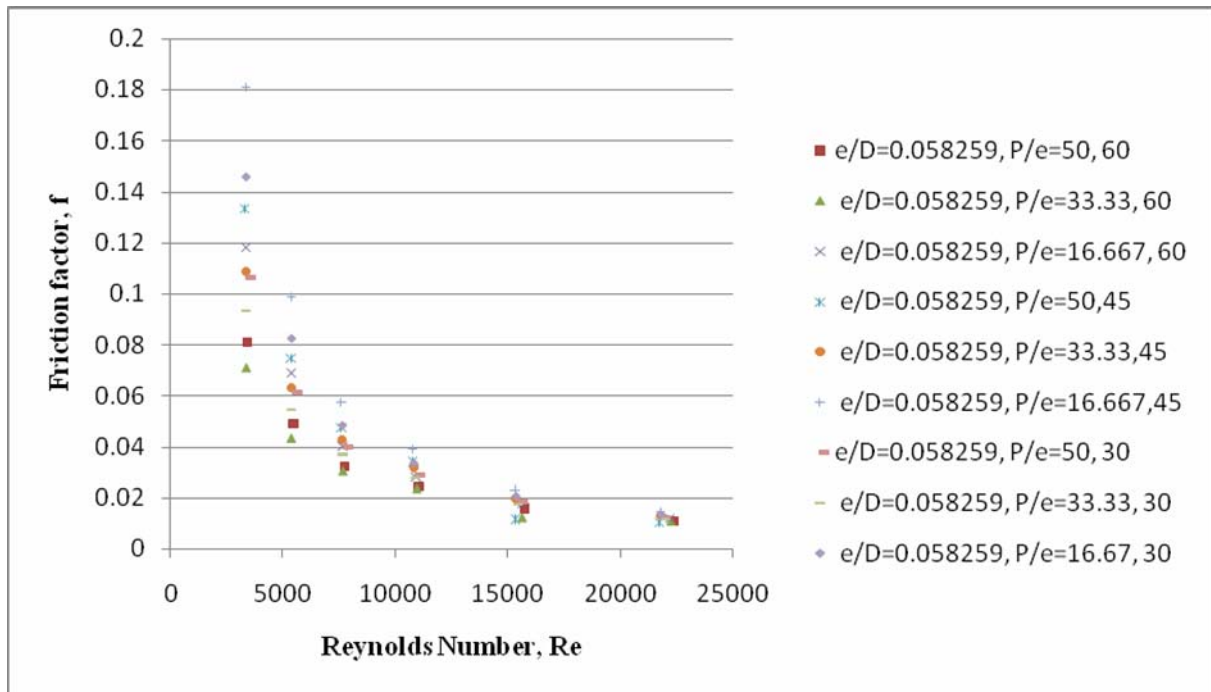


Figure 13. Variation of relative roughness height ($e/D=0.058259$) on friction factor

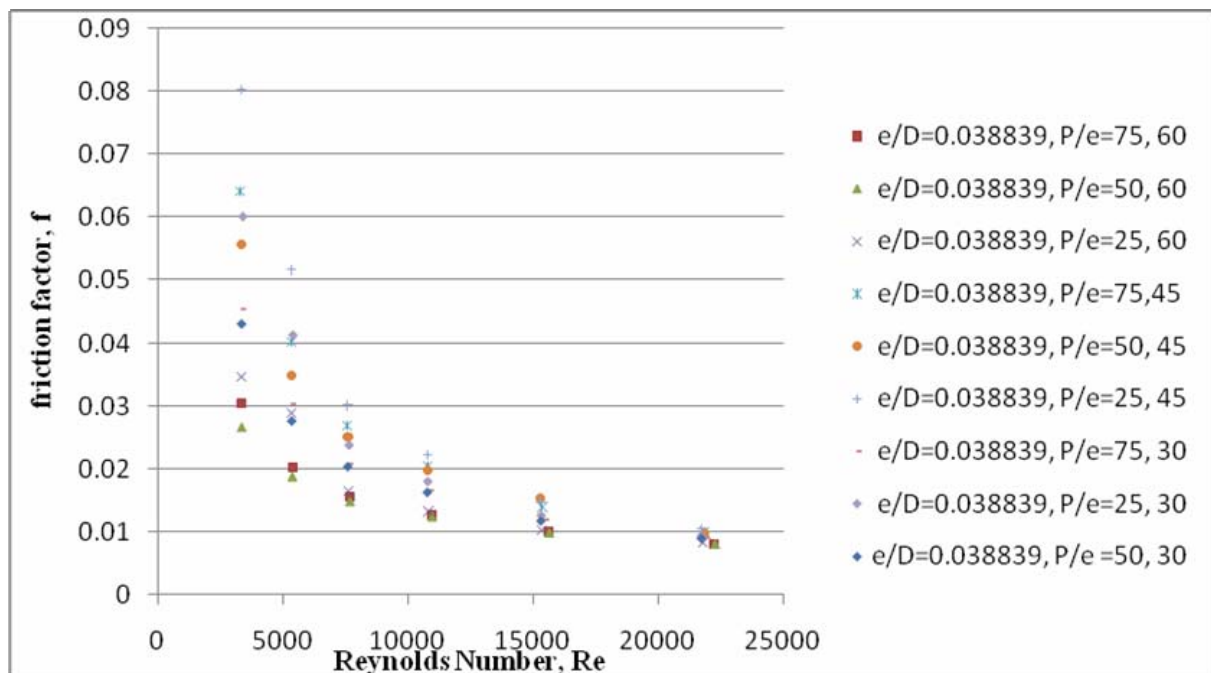


Figure 14. Variation of relative roughness height ($e/D=0.038839$) on friction factor

5.2.3 Effect of angle of attack (α)

The variation of friction factor with the angle of attack for different Reynolds number is shown in Figure 17. It has been observed that the initially friction factor increase and then decreases with angle of attack and maximum value of it lies at 45° . The reason for this phenomenon may be separation of flow resulting from the presence of M shape continuous ribs.

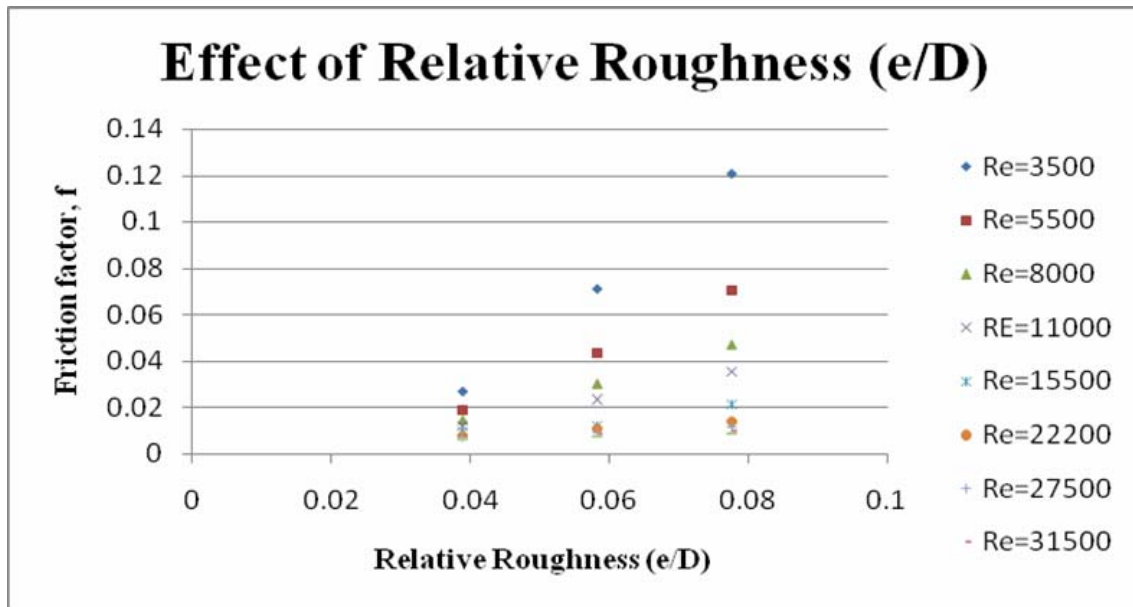


Figure 15. Effect of relative roughness height (e/D) on friction factor

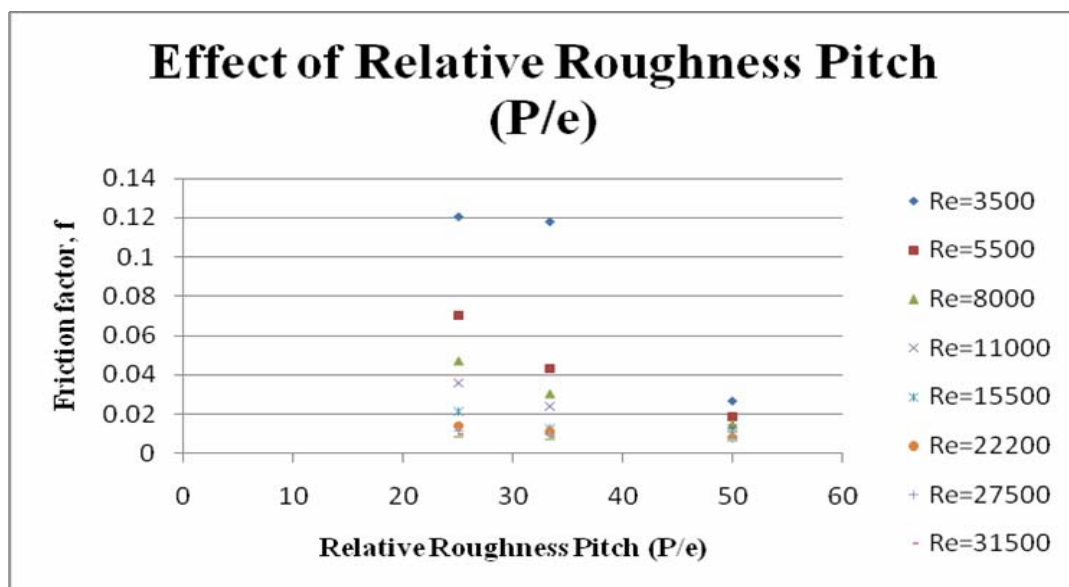


Figure 16. Effect of relative roughness pitch (P/e) on friction factor

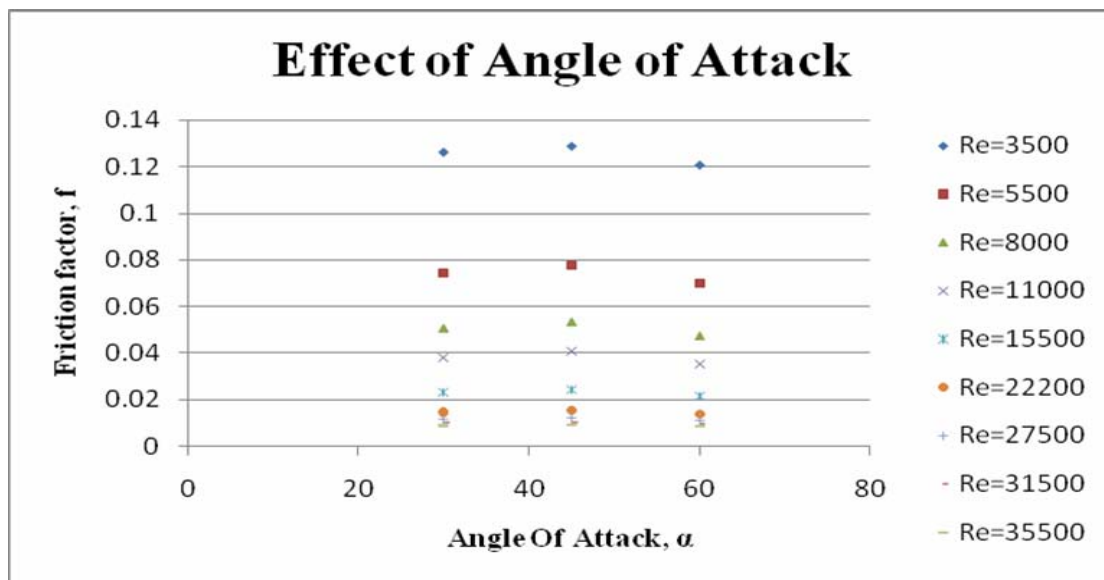


Figure17. Effect of angle of attack (α) on friction factor

6. Conclusion

After carried out the detailed experimental investigation, it has been studied that the heat transfer and friction factor characteristics of solar air heater duct which is having M shape artificial roughness on absorber plate. It is reported that Nusselt number is increasing monotonously with the increase in Reynolds number. On the other hand, friction factor also increased which leads to higher pumping power. It is necessary to obtained optimum parameters for artificial roughness M shape geometry. It has been observed that maximum heat transfer occurred at 0.07769 (e/D), 25 (P/e) and 60° while maximum friction factor occurs at 0.07769 (e/D), 25 (P/e) and 45° . A maximum heat transfer enhancement due to presence of artificial roughness has been found about 1.7-1.8 times as compared to smooth plate.

Acknowledgements

This work is technically as well as financially supported by Department of Mechanical Engineering, NIT Hamirpur and Ministry of Human Resource department.

References

- [1] Han J.C., Glicksman L.R., and Rohsenow W.M. An investigation of heat transfer and friction for rib-roughened surfaces", International Journal of Heat and Mass Transfer. 1978, 21(8), 1143-1156.
- [2] Prasad B.N., Saini J.S. Effect of artificial roughness on heat transfer and friction factor in a solar air heater. Solar Energy. 1988, 41(6), 555-560.
- [3] Prasad B.N., Saini J.S. Optimal thermohydraulic performance of artificially roughened solar air heaters, Solar Energy. 1991, 47, 91-96.
- [4] Han J.C., Glicksman L.R., Rohsenow W.M. Heat transfer and friction for rib roughened surfaces. Internatinal Journal of Heat Mass Transfer 1978, 21, 1143-56
- [5] Han J.C. Heat transfer and friction in channels with opposite rib roughened walls. Trans ASME Journal of Heat Transfer. 1984, 106, 774-81.
- [6] Han J.C., Park J.S. Developing heat transfer in rectangular channel with rib turbulators. Trans ASME Journal of Heat Transfer. 1988, 31, 183-95.
- [7] Han J.C., Ou S., Park J.S., Lei C.K. Augmented heat transfer in rectangular channels of narrow aspect ratio with ribs turbulators. International Journal of Heat Mass Transfer. 1989, 32, 1619-30.
- [8] Varun, Saini R.P., Singal S.K. Investigation of thermal performance of solar air heater having roughness elements as a combination of inclined and transverse ribs on absorber Plate. Renewable Energy. 2008, 33(6), 1398-1405.
- [9] Momin A-M.E., Saini J.S., Solanki S.C. Heat transfer and friction in solar air heater duct with V-shaped rib roughness on absorber plate. International J. of Heat and Mass Transfer. 2002, 45(16), 3383-3396.

- [10] Muluwork, K.B., Saini, J.S., and Solanki, S.C., "Studies on discrete rib roughened solar air heaters", In proceedings of National Solar Energy Convention, Roorkee, 1998, 75-84.
- [11] Muluwork, K.B., " Investigation on fluid flow and heat transfer in roughened absorber plate", Ph.D Thesis, 2000, IIT Roorkee.
- [12] Saini, S.K., Saini, R.P. Development of correlations for Nusselt number and friction factor for solar air heater with roughened duct having arc-shaped wire as artificial roughness. *Solar Energy*. 2008, 82(12), 1118-1130.
- [13] Aharwal K.R, Gandhi B.K, Saini J.S. Heat transfer and friction characteristics of solar air heater duct having integral inclined discrete ribs on absorber plate. *International Journal of Heat and Mass Transfer*. 2009, 92, 5970-5977.
- [14] Karwa R., Solanki S.C., Saini J.S. Heat transfer coefficient and friction factor correlations for the transitional flow regime in rib roughened rectangular ducts. *International J. of Heat and Mass Transfer*. 1999, 42(9), 1597-1615.
- [15] Karwa R., Solanki S.C., and Saini J.S. Thermo-hydraulic performance of solar air heaters having integral chamfered rib-groove roughness on absorber plates. *Energy*. 2001, 26,161-176.
- [16] Karmare S.V., Tikekar A.N. Heat transfer and friction factor correlation for artificially roughened duct with metal grit ribs. *International Journal of Heat and Mass Transfer*. 2007, 50, 4342-4351.
- [17] Jaurker A.R., Saini J.S., and Gandhi B.K. Heat transfer coefficient and friction characteristics of rectangular solar air heater duct using rib-grooved artificial roughness. *Solar Energy*. 2006, 80(8), 895-907.
- [18] Layek A., Saini J.S., and Solanki S.C. Heat transfer and friction characteristics for artificially roughened ducts with compound turbulators. *International Journal of Heat and Mass Transfer*. 2007, 50(23-24), 4845-4854.
- [19] Verma S.K., Pasad B.N. Investigation of optimal thermo hydraulic performance of artificially roughened solar air heaters. *Renewable Energy*. 2000, 20, 19-36.
- [20] Saini R.P., Verma J. Heat transfer and friction factor correlations for duct having dimple-shape artificial roughness for solar air heaters. *Energy* 2008, 33,1277-87.
- [21] Karmare S.V., Tikekar A.N. Analysis of fluid flow and heat transfer in a rib grit roughened surface solar air heater using CFD. *Solar Energy* 2010, 84, 409-417.
- [22] Bopache S.B., Tandale M.S. Experimental investigations on heat transfer and frictional characteristics of a turbulators roughened solar air heater duct. *International Journal of Heat and Mass Transfer*. 2009, 52, 2834-2848.
- [23] Bhushan B., Singh R. Nusselt number and friction factor correlations for solar air heater duct having artificially roughened absorber plate. *Solar Energy* 2011, 85, 1109-1118.
- [24] Promvong P., Thianpong C. Thermal performance assessment of turbulent channel flows over different shaped ribs. *International Communication in Heat and Mass Transfer*. 2008, 35, 1327-1334.
- [25] Kumar S., Saini R.P. CFD based performance analysis of a solar air heater duct provided with artificial roughness. *Renewable Energy*. 2009, 34, 1285-1291.
- [26] Lee D.H., Rhee D.H., Kim K.M., Cho H.H., Moon H.K. Detailed measurement of heat/mass transfer with continuous and multiple V-shaped ribs in rectangular channel. *Energy*. 2009, 34, 1770-1778.
- [27] Eiamsa-ard S., Seemawute P., Wongcharee K. Influences of peripherally –cut twisted tape insert on heat transfer and thermal performance characteristics in laminar and turbulent tubes flows *Experimental Thermal and Fluid science*. 2010, 34, 711-719.
- [28] Promvong P., Chompookham T., Kwankaomeng S., Thianpong C. Enhanced heat transfer in triangular ribbed channel with longitudinal vortex generators. *Energy Conversion and Management* 2010, 51, 1242-1249.
- [29] Aharwal K.R., Gandhi B.K., Saini J.S. An experimental investigation of heat transfer and fluid flow in rectangular duct with inclined discrete ribs", *International journal of Energy and Environment* 2010, .1, 987-998.
- [30] Hans V., Saini R.P., Saini J.S. Heat transfer and friction factor correlations for a solar air heater duct roughened artificially with Multiple V-ribs. *Solar Energy*. 2010, 84, 898-911.
- [31] Mittal, M.K., Varun, Saini R.P., Singal S.K. Effective efficiency of solar air heaters having different types of roughness on absorber plate. *Energy*.2007, 32(5), 739-745.

- [32] ASHRAE standard 93-77 Method of testing of determines thermal performance of solar air heater, New York 1977; 1-34.
- [33] Kline S.J., McIntock F.P. Describing uncertainties in single sample experiments. Mech. Engg. 1953, 75, 3-8.



Sachin Chaudhary has been graduated in Mechanical Engineering in 2008 and after that completed his M.Tech in 2011 from NIT Hamirpur (India) in Thermal Engineering specialization with Computational Fluid Dynamics and Heat Transfer. His area of interest is Heat Transfer, Solar Energy, Refrigeration and Air Conditioning and Fluid Mechanics.
E-mail address: sachin.chaudhary309@gmail.com



Varun has been graduated in Mechanical Engineering in 2002 and after that completed his M.Tech in Alternate Hydro Energy Systems in 2004 from IIT Roorkee (India). He has completed his doctorate in 2010 from NIT Hamirpur. He is presently working as Asstt. Professor in Department of Mechanical Engineering at National Institute of Technology, Hamirpur, India. His area of interest is Solar Air Heater, Life Cycle Assessment and Heat Transfer. He has been published more than 40 papers in International / National Journals.
E-mail address: varun7go@gmail.com



Manish Kumar Chauhan has been graduated in Mechanical Engineering in 2009 and after that completed his M.Tech in 2011 from NIT Hamirpur (India) in Thermal Engineering specialization with Computational Fluid Dynamics and Heat Transfer. He is presently working as Asstt. Professor in Department of Mechanical Engineering at College of Engineering Roorkee, Roorkee (U.K.), India. His area of interest is Fluid Mechanics, Heat Transfer, Thermal Engg., Solar Energy, Life Cycle Assessment and Non-conventional Energy Sources. He has been published more than 2 papers in International / National Journals.
E-mail address: manishku.25@gmail.com